

# Beam Energy Scan on Hypertriton Production and Lifetime Measurement at RHIC STAR

Yuhui Zhu (for the STAR Collaboration)<sup>1</sup>

Shanghai Institute of Applied Physics, 201800, Shanghai, China

---

## Abstract

We report preliminary results on  ${}^3_{\Lambda}\text{H}$  production in Au+Au collisions at RHIC at  $\sqrt{s_{\text{NN}}} = 7.7, 11.5, 19.6, 27, 39, \text{ and } 200$  GeV. The beam energy dependence of strangeness population factor  $\frac{{}^3_{\Lambda}\text{H}/{}^3\text{He}}{\Lambda/p}$  is shown and the result indicates that  $\frac{{}^3_{\Lambda}\text{H}/{}^3\text{He}}{\Lambda/p}$  has an increasing trend with  $1.7\sigma$  significance. The hypertriton lifetime combining the above Au+Au collision data set is measured to be  $123 \pm_{26}^{26}$  (stat)  $\pm 10$ (sys)ps.

---

## 1. Introduction

The hyperon-nucleon(Y-N) interaction is of great physical interest because it introduces a new quantum number strangeness in ordinary nuclear matter. It is predicted to be the decisive interaction in some high-density matter systems, such as neutron stars [1]. The Relativistic Heavy Ion Collider, RHIC, provides an ideal laboratory to study the Y-N interaction because hyperons and nucleons are abundantly produced in high energy nucleus-nucleus collisions.

The lifetime and decay modes of  ${}^3_{\Lambda}\text{H}$ , the lightest hypernucleus, which consists of a proton, a neutron and the lightest hyperon  $\Lambda$ , provide valuable insights into the Y-N interaction.

The strangeness population factor  $S_3$ , defined as  $\frac{{}^3_{\Lambda}\text{H}/{}^3\text{He}}{\Lambda/p}$ , is a good representation of the local correlation between baryon number and strangeness [2]. It is predicted that  $S_3$  has a different behavior in Quark-Gluon Plasma (QGP) and pure hadron gas [3, 4] thus can be used as a tool to distinguish QGP from a pure hadronic phase.

The RHIC beam energy scan program in 2010-2011 allowed STAR to collect data for Au+Au collisions over a broad range of energies. This provides an opportunity to study the beam energy dependence of  $S_3$ . In addition, with increased statistics of present datasets, an improved result of the lifetime measurement of the hypertriton can be obtained. To get an even better statistics, datasets are combined in the lifetime measurement.

## 2. Analysis Details

In this analysis, the  ${}^3_{\Lambda}\text{H}$  is reconstructed via the decay channel  ${}^3_{\Lambda}\text{H} \rightarrow {}^3\text{He} + \pi^-$  and its decay candidates are identified by their ionization energy loss  $dE/dx$  using the STAR detector Time

---

<sup>1</sup>A list of members of the STAR Collaboration and acknowledgements can be found at the end of this issue.

21 Projection Chamber (TPC)[6]. The TPC covers full azimuthal angle and has a good charged  
 22 particle identification ability in the pseudorapidity range from -1.0 to 1.0.

23 We define  $dE/dx^{\text{data}}$  and  $dE/dx^{\text{Bichsel}}$  separately as the  $dE/dx$  of the detected particle and  
 24 its theoretical value. Then we use the quantities  $Z = \ln(dE/dx^{\text{data}}) - \ln(dE/dx^{\text{Bichsel}})$ [7] and  
 25  $n\sigma_\pi = (\ln(dE/dx^{\text{data}}) - \ln(dE/dx^{\text{Bichsel}}))/\sigma_\pi$  ( $\sigma_\pi$  is the  $dE/dx$  resolution of  $\pi$ )[8] separately for  
 26  ${}^3\text{He}$  and  $\pi^-$  identification. The cuts:  $|Z| < 0.2$  and  $|n\sigma_\pi| < 2$  are applied. In addition, strict  
 27 topology cuts: DCA (distance of closest approach to the collision vertex)  $< 1$  cm and rigidity  
 28 (momentum/charge)  $> 1\text{GeV}/c$ , which can avoid contamination from beam-pipe knocked-out  
 29  ${}^3\text{He}$  and other particles, are also used. With all the cuts applied,  ${}^3\text{He} + {}^3\overline{\text{He}}$  can be identified very  
 30 well. We apply the same PID method in each energy.

31 We obtain the  ${}^3_\Lambda\text{H}$  signal by calculating the invariant mass of its daughters:  ${}^3\text{He}$  and  $\pi^-$ .  
 32 The background invariant mass curve is constructed by rotating one of the daughters (in this  
 33 analysis  $\pi$ ) by 180 degrees in azimuthal angle. This is used to accurately represent the combi-  
 34 natorial background[2]. Further corrections for detector acceptance and inefficiency in particle  
 35 identification have been made to both  ${}^3_\Lambda\text{H}$  and  ${}^3\text{He}$  yields using the STAR embedding simulation  
 36 method[9].

### 37 3. Results and Discussions

#### 38 3.1. Hypertriton Production

39 We successfully reconstruct  ${}^3_\Lambda\text{H} + {}^3\overline{\Lambda}\text{H}$  signals at different energies. Figure 1 shows the invari-  
 40 ant mass distribution of signals from all the beam energies. The background shape is fitted by  
 41 a double exponential function:  $f(x) \propto \exp(-\frac{x}{p_1}) - \exp(-\frac{x}{p_2})$ , where  $p_1$  and  $p_2$  are fit parameters.  
 42 The signal is then fitted by adding a gaussian function to the background, and its yield is derived  
 43 from bin counting within mass range  $[2.986, 2.996]\text{GeV}/c^2$ . The peak has a significance of  $9.6\sigma$ .

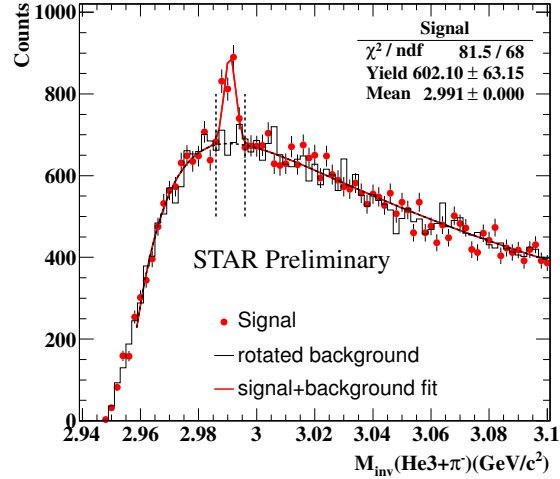


Figure 1: (Color online)  ${}^3_\Lambda\text{H} + {}^3\overline{\Lambda}\text{H}$  with all datasets combined. Vertical dashed lines represent the mass range we use for bin counting of  ${}^3_\Lambda\text{H}$  yield.

44 The V0 ( ${}^3_{\Lambda}\text{H}$  vertex) cuts, including the DCA between  ${}^3\text{He}$  and  $\pi$ , separate DCA of the  ${}^3_{\Lambda}\text{H}$   
 45 and  $\pi$  to the collision vertex, and decay length of the  ${}^3_{\Lambda}\text{H}$  are separately optimized in each dataset.

### 46 3.2. Strangeness Population Factor

47 The  $({}^3_{\Lambda}\text{H} + {}^3_{\Lambda}\bar{\text{H}})/({}^3\text{He} + {}^3\bar{\text{He}})$  ratio is calculated by dividing efficiency corrected  ${}^3\text{He} + {}^3\bar{\text{He}}$   
 48 and  ${}^3_{\Lambda}\text{H} + {}^3_{\Lambda}\bar{\text{H}}$  yields within  $p_{\text{T}}$  range [2,5]GeV/c. The  $\Lambda/p$  ratio is extracted from [5]. The  
 49 beam energy dependence of efficiency corrected  $S_3$  is shown in Fig. 2 left panel. Two model  
 50 calculations from [3, 4] are also included in the plot. From the trend of data points, it is hard to  
 51 draw a conclusion directly. Therefore, a quantitative calculation is done by applying a zero-order  
 52 and first-order fit to the data points, as shown in Fig. 2 right panel. From the fit results, we can  
 53 give a statement that  $S_3$  increases with increasing beam energy with  $1.7\sigma$  significance.

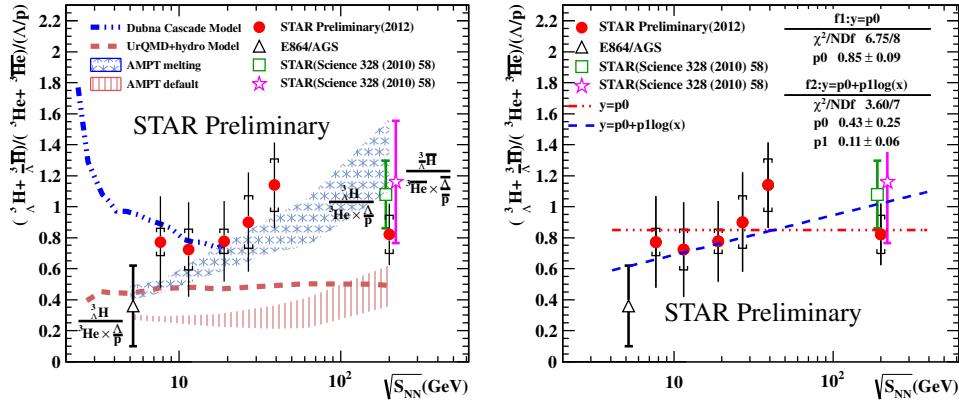


Figure 2: (Color online)(Left) Beam energy dependence of  $S_3$ . Lines and shadows: model calculation results. Markers: experimental results. (Right) Quantitative fit of the data points.

### 54 3.3. Lifetime Measurement

55 The hypertriton yield obeys the radioactive decay formula:  $N(t) = N(0)e^{-t/\tau} = N(0)e^{-1/(\beta\gamma c\tau)}$   
 56 ( $\tau$ :lifetime,  $1/{}^3_{\Lambda}\text{H}$  decay length). We reconstruct  ${}^3_{\Lambda}\text{H} + {}^3_{\Lambda}\bar{\text{H}}$  signals in four  $1/(\beta\gamma)$  bins: [2cm,5cm],  
 57 [5cm,8cm], [8cm,11cm], [11cm,41cm]. The lifetime parameter is then extracted by fitting the  
 58 decay formula to the 4 data points. Asymmetric statistical errors are calculated by doing  $\chi^2$  esti-  
 59 mation as shown in the inner panel in the left panel of Fig. 3. The result is  $123 \pm_{22}^{26}(\text{stat}) \pm 10(\text{sys})$   
 60 ps. As a comparison, STAR 2010  ${}^3_{\Lambda}\text{H}$  lifetime measurement [2] and the STAR 2010+2012 com-  
 61 bined results are also provided. The current measurement is consistent with the STAR 2010  
 62 measurement within  $1.5\sigma$  and is statistically improved.

63 We consider two kinds of sources for systematic study: 1. choice of V0 topology cuts; 2.  
 64 choice of bin width and invariant mass range. These effects contribute to the final systematic  
 65 error. Additional sources of loss, like the interaction between  ${}^3_{\Lambda}\text{H}$  and material (air+detector) are  
 66 also considered, which can be neglected due to its less than 1.5% effect.

67 As a further cross-check,  $\Lambda$  is reconstructed via the  $\Lambda \rightarrow p + \pi^-$  decay channel. We use  
 68 exactly the same method to obtain the  $\Lambda$  lifetime and the result is  $260 \pm 1$  ps which is consistent

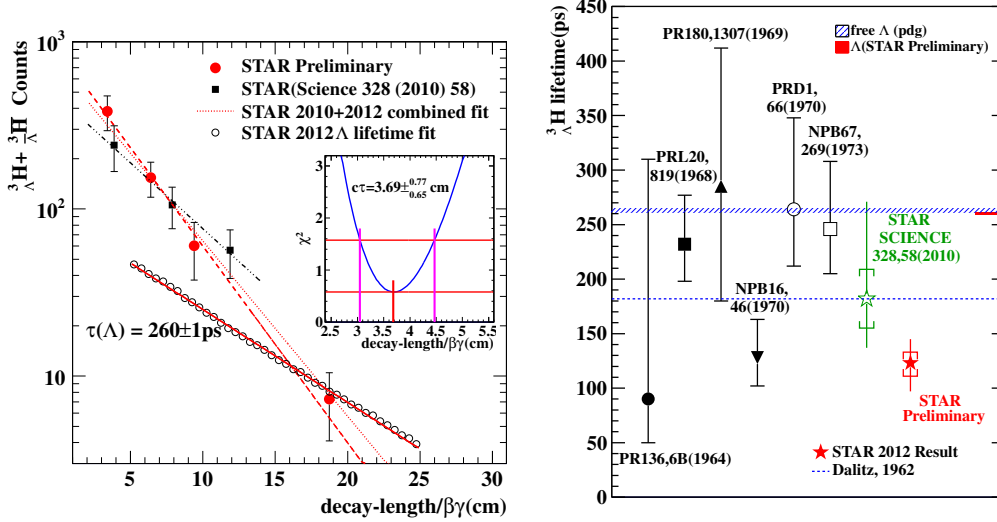


Figure 3: (Color online)(Left)  ${}^3_{\Lambda}\text{H} + {}^3_{\Lambda}\bar{\text{H}}$  yield versus  $c\tau$ . STAR 2012 (solid red circles) and 2010 (solid black squares) measurements are shown.  $\Lambda$  lifetime (open black circles) is shown as a cross-check. (Left inner pad)  $\chi^2$  estimation for calculating lifetime statistical errors. (Right) Summary of  ${}^3_{\Lambda}\text{H}$  lifetime measurements till now.

69 with the  $\tau = 263 \pm 2$  ps compiled by the Particle Data Group [10]. There have been several  
70 measurement results of  ${}^3_{\Lambda}\text{H}$  lifetime till now. We summarize the lifetime values from all the  
71 measurements till now in the right panel of Fig. 3.

#### 72 4. Summary

73 We present the STAR preliminary analysis on  ${}^3_{\Lambda}\text{H}$  production in RHIC Au+Au collisions at  
74  $\sqrt{s_{\text{NN}}} = 7.7, 11.5, 19.6, 27, 39,$  and  $200$  GeV. The combined  ${}^3_{\Lambda}\text{H} + {}^3_{\Lambda}\bar{\text{H}}$  signal is obtained with  $9.6\sigma$   
75 significance. The beam energy dependence of strangeness population factor  $\frac{{}^3_{\Lambda}\text{H}/{}^3\text{He}}{\Lambda/p}$  is presented  
76 and the result indicates that  $S_3$  increases with increasing beam energy with  $1.7\sigma$  significancy. A  
77 statistically improved  ${}^3_{\Lambda}\text{H}$  lifetime:  $123 \pm_{22}^{26}(\text{stat}) \pm 10(\text{sys})$  ps, is also presented.

78 This work was supported in part by the National Natural Science Foundation of China under  
79 contract Nos. 11035009, 11220101005, 11275250 and 10905085.

#### 80 References

- 81 [1] J. M. Lattimer, M. Prakash, *Science* 304, 536 (2004).  
82 [2] B. I. Abelev, *et al.* (STAR Collaboration), *Science* 328, 58 (2010).  
83 [3] S. Zhang *et al.*, *Phys. Lett. B.* 684, 224 (2010).  
84 [4] J. Steinheimer *et al.*, *Phys. Lett. B* 714, 85 (2012).  
85 [5] A. Andronic *et al.*, *Phys. Lett. B* 697, 203 (2011).  
86 [6] M. Anderson *et al.*, *Nucl. Instrum. Meth. A* 499, 659 (2003).  
87 [7] B. I. Abelev *et al.*, *Phys. Rev. C* 79,034909 (2009).  
88 [8] M. Shao *et al.*, *Nucl. Instrum. Meth. A* 558, 419 (2006).  
89 [9] J. Adams *et al.*, *Phys. Rev. Lett.* 98, 062301 (2007).  
90 [10] C. Amsler *et al.*, *Phys. Lett. B* 667, 1 (2008).